COUPLING CHARACTERISTICS OF ASYMMETRIC CFRP OPEN CHANNEL STRUCTURE FOR ARTIFICIAL FOOT

Ayumi YAMAMOTO[1], Shota KAGE[1] Junji NODA[1]

[1] Department of Biomechanical and Human Factors Engineering, Kindai University, Kinokawa, Japan

Keywords: *coupling, asymmetric, finite element analyses*

ABSTRACT

The shock-absorbing ability of the artificial foot part is very important for artificial foot users in terms of preventing injuries and maintaining the durability of the artificial foot. The human foot absorbs the shock of weight-bearing by means of the plantar arch and internal rotation of the tibia. However, there are no artificial feet that imitate the internal rotation of the tibia due to the deformation characteristics of the material. Therefore, we aimed to develop an artificial foot part that can imitate the internal rotation angle of an able-bodied person in the standing posture only by material deformation. By performing FEM analysis with various stacking sequences, we found a stacking sequence that provides high stiffness and a twist angle. Furthermore, we found effective stiffness and twist angle by inserting a slit in the structure to obtain the required twist angle.

1 INTRODUCTION

Artificial feet enable people with missing lower limbs to regain their daily lives by compensating for the roles they have lost. The human foot absorbs the shock of weight-bearing by means of the plantar arch and internal rotation of the tibia[1)]. The shock-absorbing capacity of the artificial foot part is very important for artificial foot users to prevent injuries and to maintain the durability of the artificial foot. Currently, some artificial foot parts are composed of many mechanical elements, while others use the deformation properties of materials. Artificial feet composed of many mechanical elements can imitate the role of internal rotation, but they have problems of complexity, weight, cost, and durability. Artificial feet that use the deformability of materials have the advantages of low cost, durability, and ease of use, but none of them can imitate shock absorption by internal rotation. We focused on the coupling characteristics of asymmetrically stacked CFRP to imitate the internal rotation of the foot without the use of mechanical elements. In the current design of structures using CFRP, the coupling property has been academically discovered but is avoided, and its practical application is extremely difficult, so few products have been developed. Although CFRP is widely used in the design of artificial foot parts, it is only focused on the aspect of high stiffness, and few studies have focused on the coupling properties that depend on the stacking sequences, which is innovative research in material mechanics and artificial foot design science. Therefore, we measured the amount of internal rotation of the tibia of an able-bodied person's dominant foot during unloading and loading and investigated the angle of internal rotation with loading. We found that the tibia was internally rotated by 4.1°. Based on these results, we aimed to develop an artificial foot that could withstand 600 N, if the twist angle generated by the coupling characteristics of the asymmetric CFRP layer was 4.1° and that the weight of the artificial foot user was 60 kg. The coupling characteristics of the asymmetric layer cannot be used in the artificial foot part, which is limited in space, without a flat plate. We proposed a U-shaped structure, which is one of the aperture structures, but the U-shaped structure could not solve the tilt of the loaded part, so we proposed an S-shaped structure, which is a combination of two U-shaped structures. In this study, we evaluated the method to achieve a twist of 2.05° while maintaining the rigidity of the U-shaped structure, which is a part of the S-shaped structure, by finite element analysis.

2 MAX DEFORMATION AND TWIST ANGLE DUE TO CHANGES IN STACKING SEQUENCES

2.1 BOUNDARY CONDITIONS FOR ANALYSIS OF DIFFERENT STACKING SEQUENCES

Static structural analysis was performed using the general-purpose finite element method program ANSYS ver. 2021 R2. Table 1 shows the material property values for orthogonal anisotropy of the CFRP used in the analysis.

Table 1: Orthotropic material properties

Young's modulus, GPa	E_{11}	133
	E_{22}	8.96
	E_{33}	8.96
Poisson's ratio	ν_{12}	0.30
	ν_{23}	0.49
	ν_{31}	0.30
Shear modulus, GPa	G_{12}	5.376
	G_{23}	4.446
	G_{31}	5.379
Thermal expansion coefficient, K^{-1}	α_1	1.15×10^{-8}
	α_2	3.76×10^{-5}
	α_3	3.76×10^{-5}

The analysis model is a U-shaped cross-sectional structure with a width of 60 mm, a height of 30 mm, and a curvature of 15 mm, as shown in Fig. 1. The thickness per layer of CFRP prepreg was 0.25 mm. Table 2 shows the stacking sequences examined in this study.

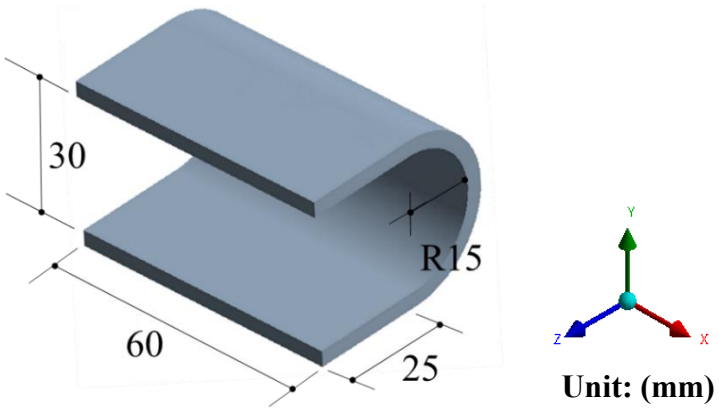

Figure 1: FEM model

Table 2: Max. deformation and twist angle of stacked sequences

No.	Num. of layer	Stacking sequences
1	14	[0/0/30/45/60/90/90/90/90/-60/-45/-30/0/0]
2		[90/90/60/45/30/0/0/0/0/-30/-45/-60/90/90]
3		[30/45/60/90/0/90/0/0/90/0/90/-60/-45/-30]

The stacking direction was 0˚ in the x-axis direction and 90˚ in the z-axis direction, and the elements were stacked from the inside. The element type was a hexahedral 8-node solit element with a mesh size of 1 mm. The yellow areas (-30,15,0) shown in Fig. 2 were fully constrained as boundary conditions to analyze the thermal deformation of the U-shaped cross section asymmetric CFRP structure. A temperature variation of -108°C from a cooling temperature of 130°C to 22°C during curing was applied.

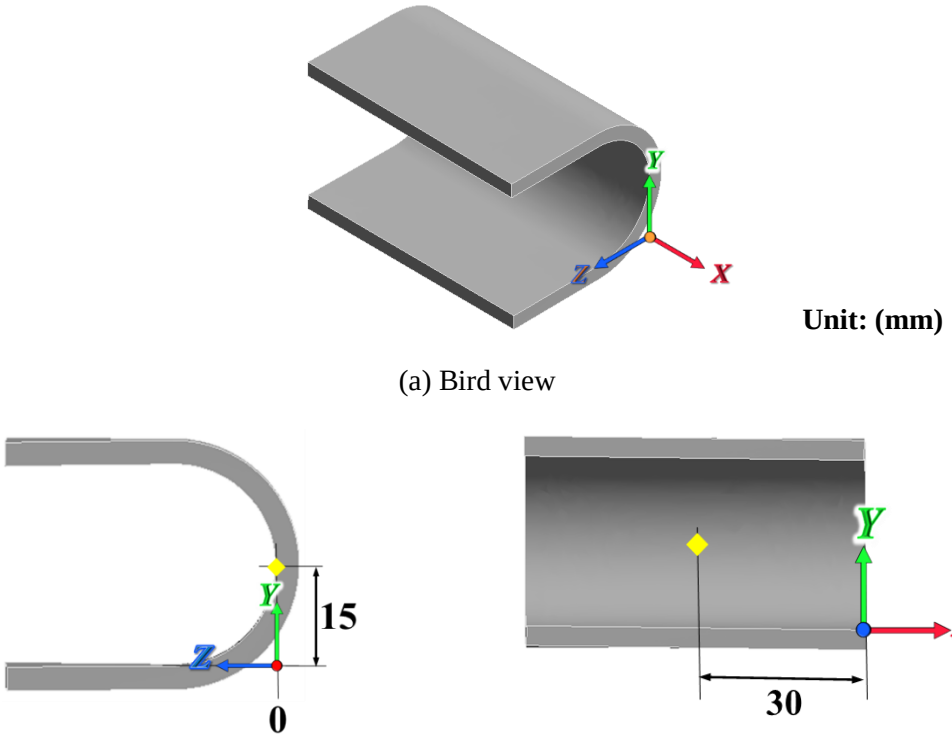

(a) Bird view

(b) *y*-*z* view

(c) *y*-*x* view

Figure 2: Thermal boundary condition

Next, a U-shaped asymmetric CFRP structure with thermally deformed cross section was subjected to bending loads. 2 green points (-20,0,27.5) and (-40,0,27.5) at the bottom shown in Fig. 3 were fully constrained, and a single point load of -600 N in the y axis direction was applied to the red point (-20,33.5,16) at the top. Bending analysis was performed. Note that both analyses were performed for large deformation.

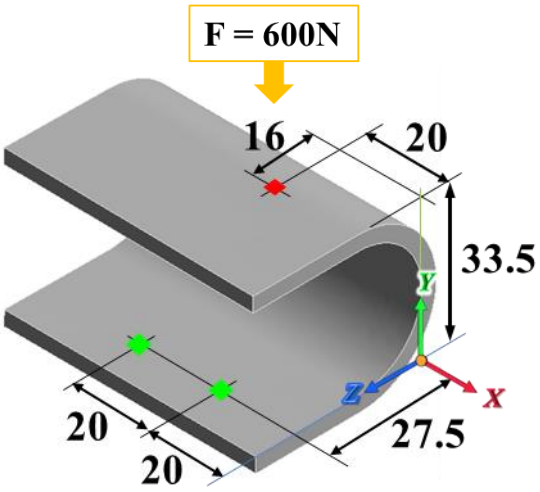

Figure 3: Load boundary condition

2.2 ANALYSIS RESULTS FOR DIFFERENT STACKING SEQUENCES

Fig. 4 shows the relationship between twist angle and max deformation for each stacking sequence. The figure shows that the rigidity increases, and the twist angle increases when the layer with the smallest lamination angle is placed on the outside and the layer with the largest lamination angle is placed on the inside. The figure shows that the twist angle did not reach the target value of 2.05˚.

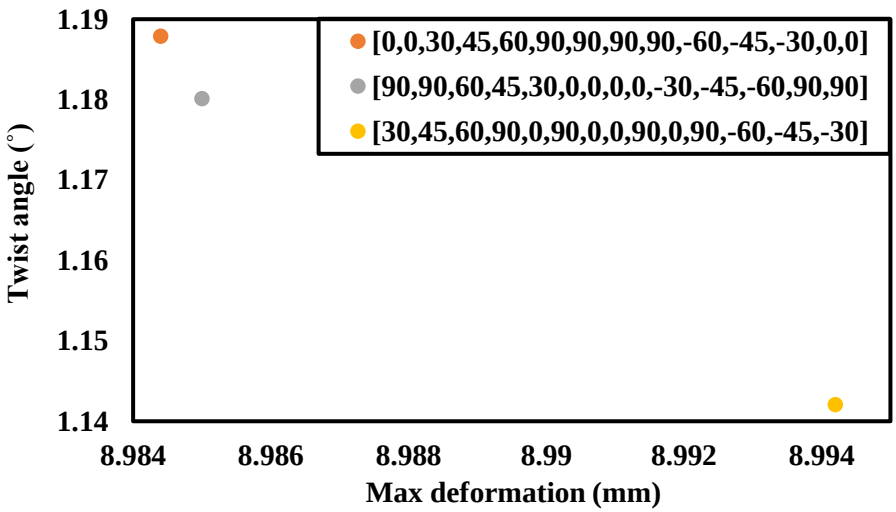

Figure 4: Twist angle – max. deformation relations

3 MAX DEFORMATION AND TWIST ANGLE DUE TO SLIT

We considered that the amount of twist could be obtained by inserting a slit in a U-shaped cross-sectional structure and evaluated the change in stiffness and twist angle depending on the type of slit.

3.1 BOUNDARY CONDITIONS FOR ANALYSIS OF SLIT MODELS

The analytical model consists of various slits in the euphemistic part of the model shown in Chapter 2. The number, width, position, and total area of slits for the various models are shown in Table 2, and the respective model diagrams are shown in Figure 5. The model names are given as number of slits (N~) _width of slits (W~) _area with slits (A~) _type of slit position (~). The mesh size was set to 1mm. The stacking sequences were twisted with the highest stiffness based on the results in Chapter 2. The mesh size was set to [0/0/30/45/60/90/90/90/90/90/60/-45/-45/-30/0/0]. The boundary conditions are the same as in Chapter 2.

Table 3: Type of slit

Model	Num. of slits	Slits width (mm)	Interval (_: slits)	Total area of slits (mm^2)
N0_W0_A0_a	0	-	-	0
N1_W20_A942_a	1	20	20_20	942
N5_W4_A942_a	5	4	7_7_6_6_7_7	942
N9_W2_A848_a	9	2	5_4_4_4_4_4_4_4_4_5	848
N10_W1_A471_a	10	1	4_4_4_4_6_6_6_4_4_4_4	471
N10_W2_A942_a	10	2	3_3_3_3_5_6_5_3_3_3_3	942
N14_W1_A660_a	14	1	3_…_3_4_3_…_3	660
N20_W0.5_A471_a	20	0.5	2_ …_2_10 _2_…_2	471
N20_W0.5_A471_b	20	0.5	2.3_…_2.3_2.4_…_2.4_2.3_…_2.3	471
N20_W0.5_A471_c	20	0.5	1_…_1_30	471
N20_W0.5_A471_d	20	0.5	30_1_…_1	471
N20_W0.5_A471_e	20	0.5	2_…_2_10	471
N20_W0.5_A471_f	20	0.5	10_2_…_2	471
N20_W1_A942_a	20	1	1.5_1.5_2_…_2_1.5_1.5	942

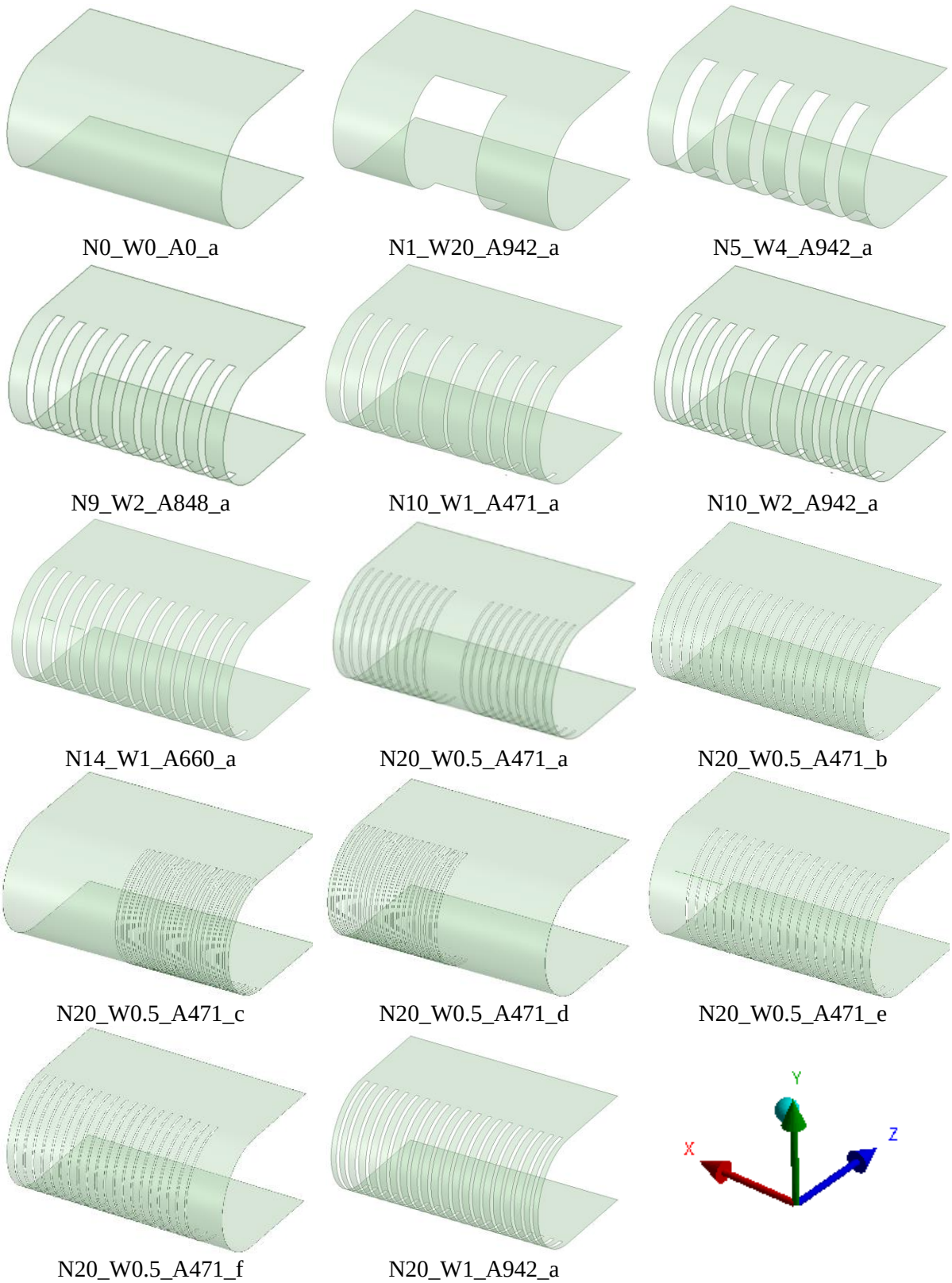

Figure 5: FEM models with slit

3.2 ANALYSIS RESULTS OF SLIT MODEL

Table 3 and Fig. 6 show the relationship between twist angle and max deformation for models with 10, 14, and 20 slits of 1 mm width. The figure shows that the max deformation and twist angle increase as the number of slits of the same width is increased.

Table 4: Max. deformation and twist angle for N10_W1_A471_a, etc.

Name	Width of slits (mm)	Num. of slits	Max deformation (mm)	Twist angle (˚)
N10_W1_A471_a	1	10	10.637	1.803
N14_W1_A660_a		14	12.647	2.106
N20_W1_A942_a		20	16.075	2.813

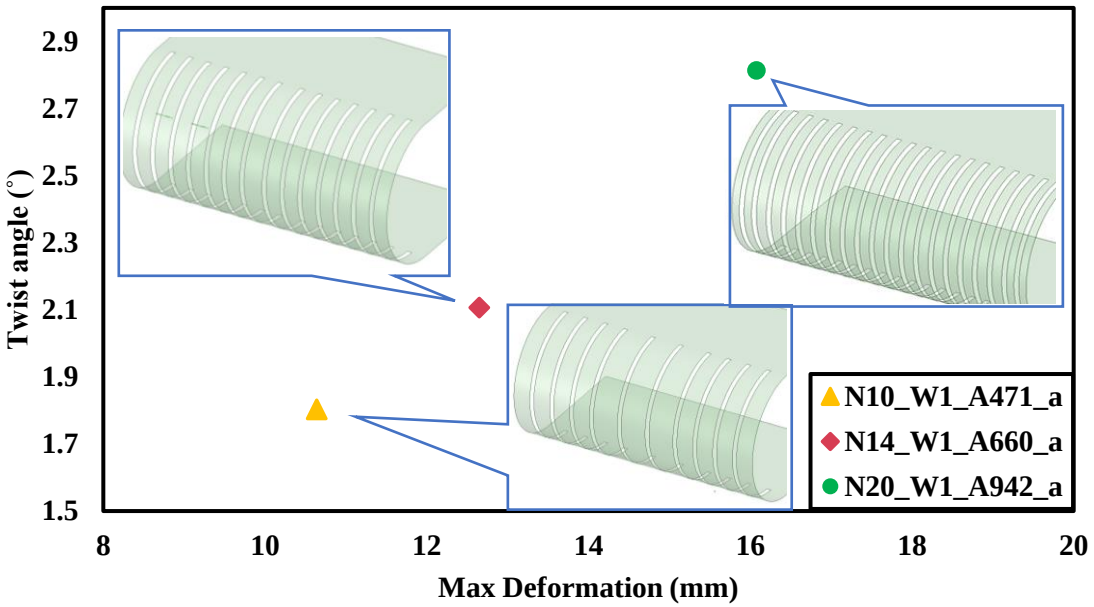

Figure 6: Twist angle – max. deformation relations for N10_W1_A471_a, etc.

Table 4, Fig. 7 shows the relationship between the twist angle and the max deformation of the model with the number of slits increased and the slit width decreased so that the hollowed-out area is the same as 942.5 mm^2.The max deformation and twist angle increase as the number of slits increases even though the hollowing out area is the same.

Table 5: Max. deformation and twist angle for N1_W20_A942_a, etc.

Name	Total area of slits (mm)	Num. of slits	Width of slits (mm)	Max. deformation (mm)	Twist angle (º)
N1_W20_A942_a	942	1	20	14.19	1.652
N5_W4_A942_a		5	4	14.75	1.88
N10_W2_A942_a		10	2	15.15	2.095
N20_W1_A942_a		20	1	16.08	2.813

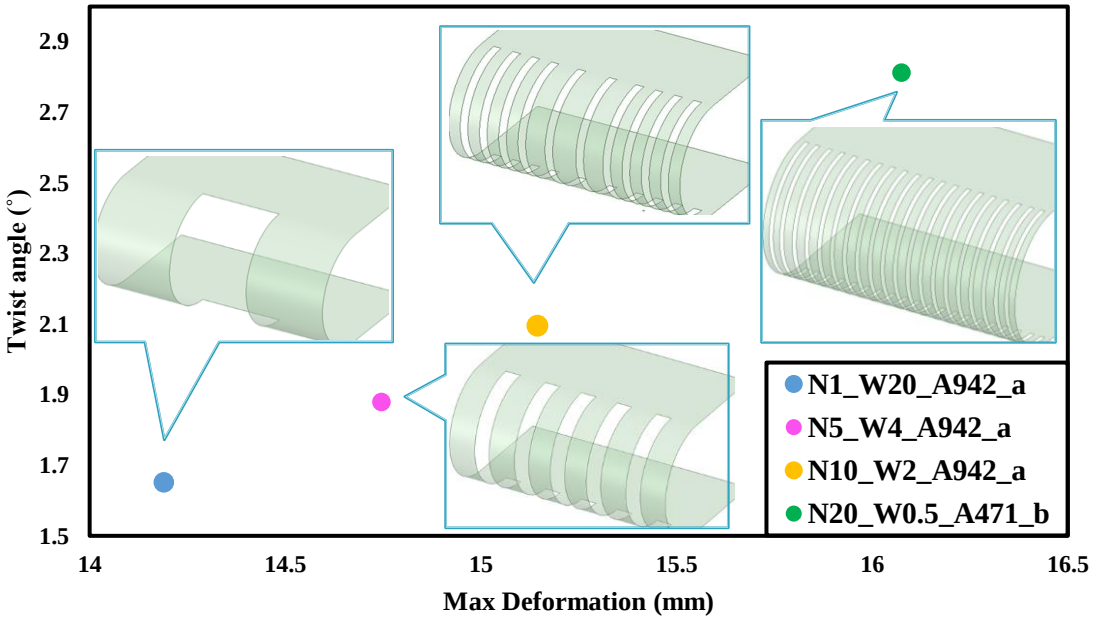

Figure 7: Twist angle – max. deformation relations for N1_W20_A942_a, etc.

Table 5, Fig. 8 shows the relationship between twist angle and max deformation for the model with increasing number of slits and decreasing hollowed-out area. The maximum deformation decreases, and the twist angle increases as the number of slits increases and the hollowed-out area decreases. From these results, it is considered possible to increase the number of slits and decrease the hollowed-out area of the U-shaped structure by decreasing the slit width to obtain the amount of twist angle while maintaining rigidity.

Table 6: Max. deformation and twist angle for N5_W4_A942_a, etc.

Model	Num. of slits	Width of slits (mm)	Total area of slits (mm^2)	Max deformation (mm)	Twist angle (˚)
N5_W4_A942_a	5	4	942	14.746	1.880
N9_W2_A848_a	9	2	848	13.353	1.977
N14_W1_A660_a	14	1	660	12.647	2.106
N20_W0.5_A471_a	20	0.5	471	9.9984	2.235

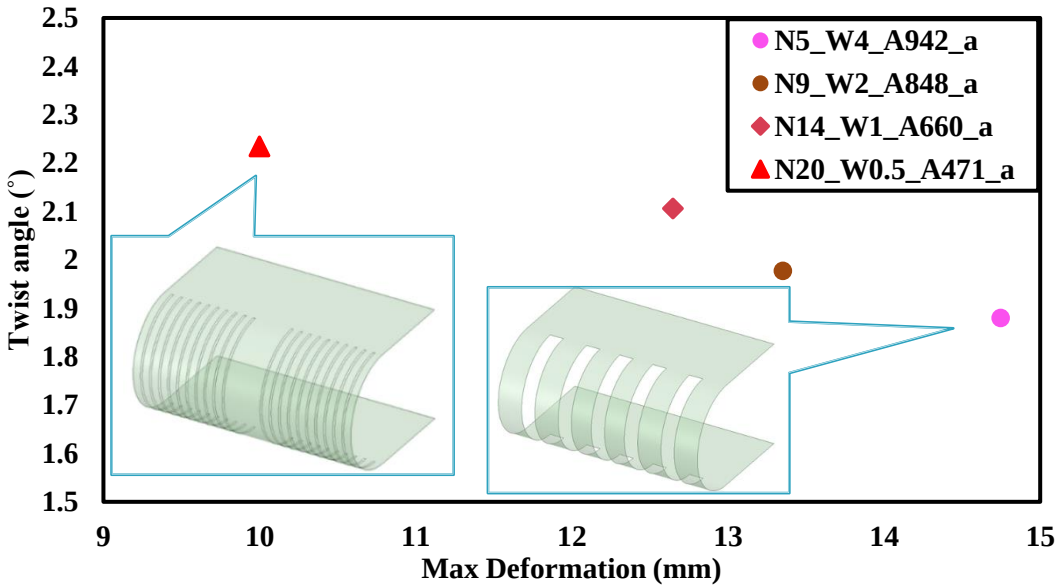

Figure 8: Twist angle – max. deformation relations for N5_W4_A942_a, etc.

Table 6 and Fig. 9 show the relationship between twist angle and max deformation for models with the same number of slits, slit width, and hollowed-out area but different slit positions. The stiffness of the U-shaped structure is considered to increase with the position of the slit, and the twist angle is considered to increase.

Table 7: Max. deformation and twist angle for N20_W0.5_A471_a, etc.

Model	Num. of slits	Width (mm)	Total area of slits (mm^2)	Interval (_ :slits)	Max deformation (mm)	Twist angle (˚)
N20_W0.5_A471_a	20	0.5	471	2_… _2_10 _2_…_2_10	9.998	2.235
N20_W0.5_A471_b				2.3_2.3_2.4_…_2.4_2.3_2.3	10.831	2.167
N20_W0.5_A471_c				1_…_1_30	11.894	1.754
N20_W0.5_A471_d				30_1_…_1	10.035	1.548
N20_W0.5_A471_e				2_…_2_10	10.191	2.221
N20_W0.5_A471_f				10_2_…_2	10.021	1.791

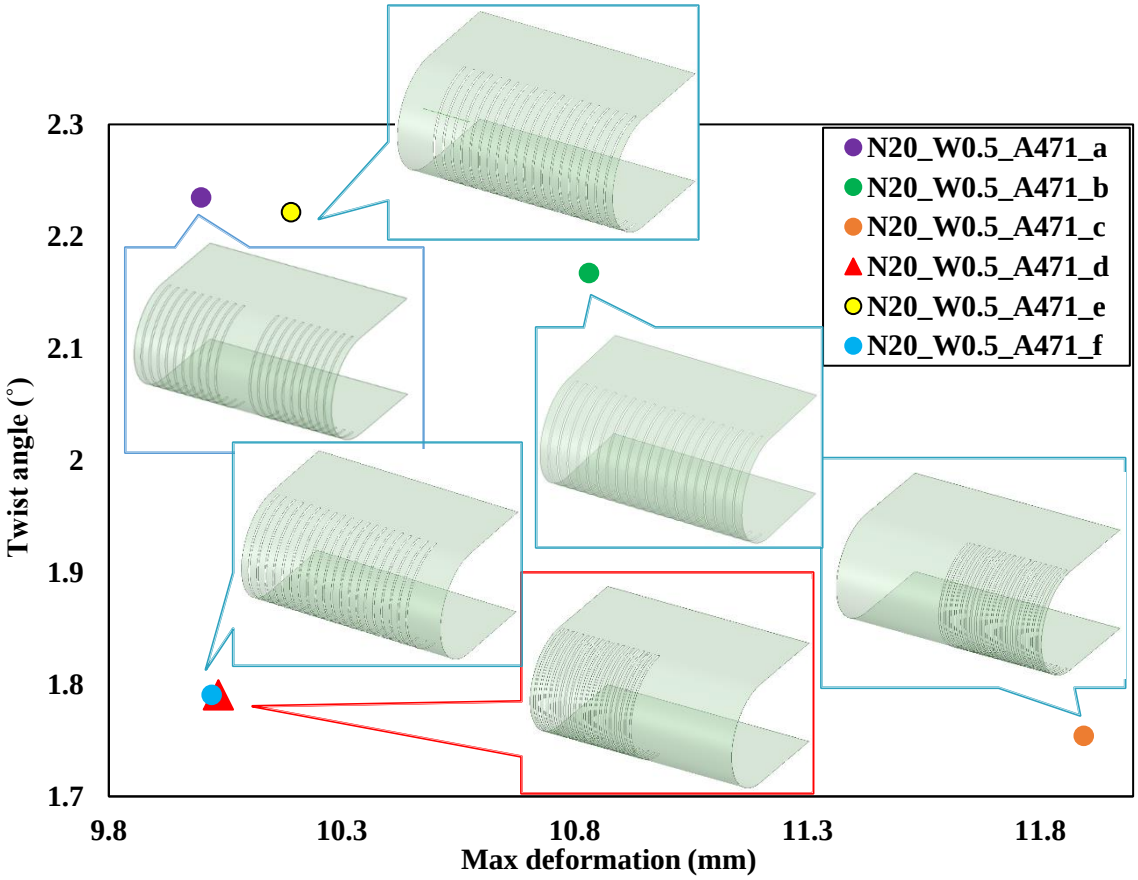

Figure 9: Twist angle – max. deformation relations for N20_W0.5_A471_a, etc.

Figure 10 (a) and (b) show contour plots of the equivalent stress distribution for each selected location for models N0_W0_A0_and N14_W1_A660_a, respectively. Figure 9(a) shows that the maximum equivalent stress is applied inside the apex of the curved section. Comparing model N0_W0_A0_a without slit and model N14_W1_A660_a with slit from (b) in Figure 10, stress is concentrated at the edge of the slit in model N14_W1_A660_a with slit, which is considered to reduce the strength of the U-shaped structure. Therefore, we believe that the strength of the U-shaped structure can be maintained by distributing the positions of the slit ends.

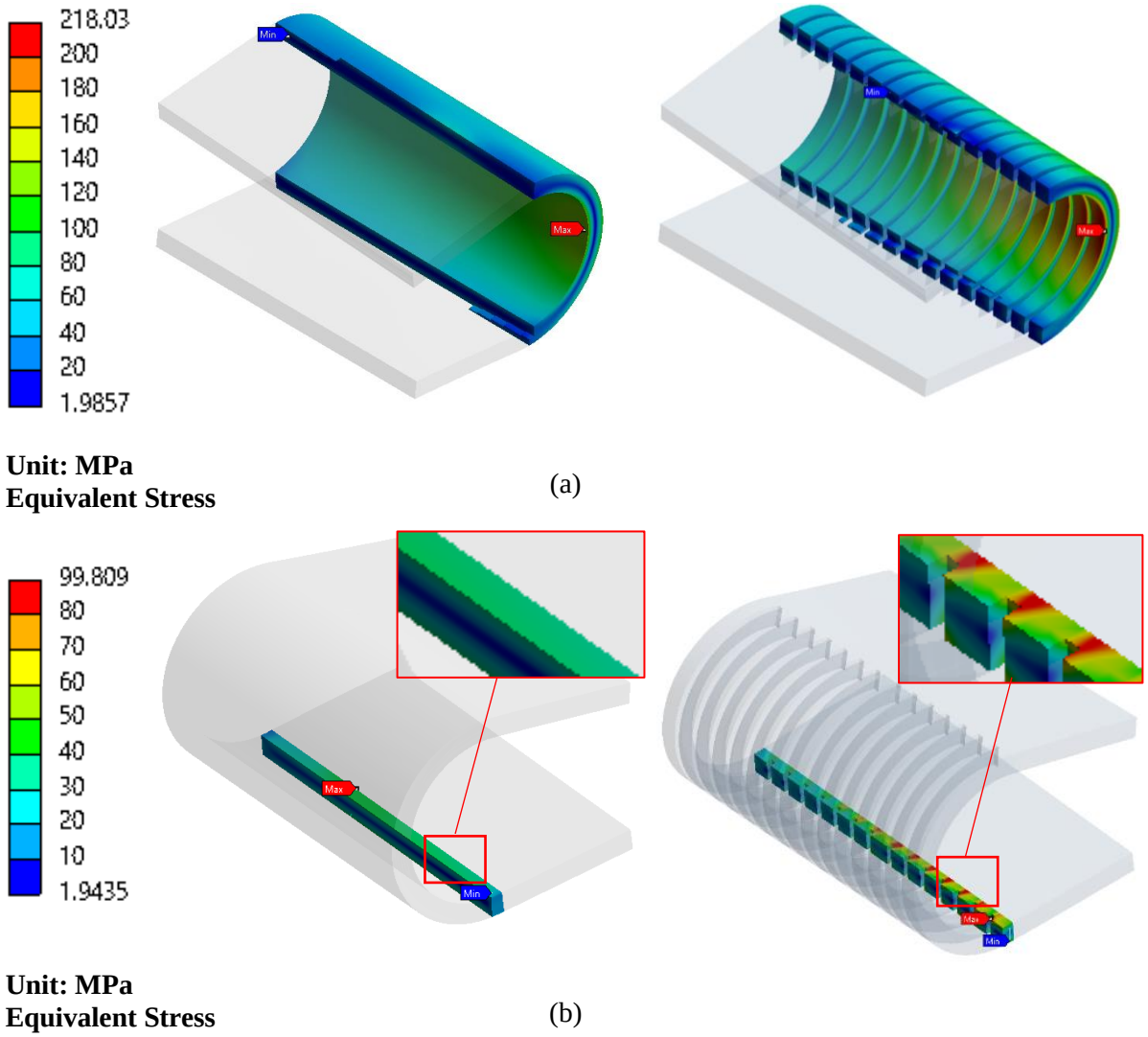

Figure 10: Equivalent stress distributions

4 CONCLUSIONS

The U-shape structure can be made rigid and twisted by increasing the number of slits and decreasing the slit width to reduce the hollowed-out area. The analysis results for Model N14_W1_A660_a with stacking sequences [0/0/0/0/30/45/60/90/90/90/90/-60/-45/-30/0/0], load points (x,y,z)=(-20,33.5,16), 14 slits, slit width 1mm, max deformation 12.647mm, torsion 2.647mm. The maximum displacement and twist angle are 12.647 mm and 2.106˚, respectively. The model N14_W1_A660_a with a slit in the U-shaped structure has stress concentrated at the edge of the slit, so the stress can be dispersed by distributing the position of the slit edge to achieve a rigid and twisting U-shaped structure. We believe that it is possible to realize a torsional U-shaped structure with high rigidity by distributing the positions of the slit ends. We will need to conduct further experiments to confirm the validity of the results of this analysis.

REFERENCES

[1] Jacquelin Perry, Judith M. Burnfield, Perry Gait Analysis Normal and Abnormal Gait Original 2nd Edition, Medical and Dental Publishing Co.